文章编号:1000-0550(2020)01-0124-14 DOI: 10.14027/j.issn.1000-0550.2019.073

沉积过程对自生黄铁矿硫同位素的约束

刘喜停[1],李安春[2],马志鑫[3],董江[4],张凯棣[2],徐方建[5],王厚杰[1]

1.中国海洋大学海洋地球科学学院,海底科学与探测技术教育部重点实验室,山东青岛 266100

2.中国科学院海洋研究所海洋地质与环境重点实验室,山东青岛 266071

3.中国地质调查局成都地质调查中心,成都 610081

4.自然资源部第一海洋研究所海洋沉积与环境地质重点实验室,山东青岛 266061

5.中国石油大学(华东)地球科学与技术学院,山东青岛 266580

摘 要 自生黄铁矿是海洋沉积物中还原态硫的主要赋存形式,其形成过程与有机质矿化相关,影响全球的C-S-Fe生物地球化学循环。自生黄铁矿硫同位素分馏主要受微生物硫酸盐还原的控制,但近期的研究成果表明局部沉积环境的改变也可以影响黄铁矿硫同位素的组成,特别是在浅海环境。在浅海非稳态沉积环境内,物理再改造和生物扰动作用,导致硫酸盐还原带内生成的硫化物被再氧化,进而影响黄铁矿的硫同位素值。浅海沉积过程容易受到古气候和海平面变化的影响,引起沉积速率的剧烈波动,导致有机质和活性铁输入的不稳定,进而影响成岩系统的开放性和硫酸盐还原速率,最终影响黄铁矿的硫同位素值。另外,沉积速率的改变还影响硫酸盐—甲烷转换带的迁移,造成有机质和甲烷厌氧氧化硫酸盐还原的相互转化,产生不同的硫同位素信号。东海内陆架泥质区为研究沉积过程对自生黄铁矿的形成及其硫同位素组成的约束机制提供了很好的研究材料。该区域有很好的沉积学研究基础,自生黄铁矿丰富、并且个别层位有生物气(甲烷为主)存在,是研究边缘海C-S-Fe循环的理想场所。

关键词 黄铁矿;硫同位素;微生物硫酸盐还原;沉积环境;东海

第一作者简介 刘喜停,男,1983年出生,博士,副教授,海洋沉积学,E-mail: liuxiting@ouc.edu.cn

中图分类号 P736.4+4 **文献标志码** A

0 引言

海洋是地球上最大的硫储库,其中硫酸盐(SO_4^{2-})是海水中硫的主要赋存形式,现代海洋中的硫酸盐平均含量达到29 mmol/L[1]。海水硫酸盐在有机质矿化的驱动下转变为硫化物进入海洋沉积物,因此海洋沉积物是硫的最主要的"汇"[2]。在稳态环境中,按照自由能大小,有机质矿化先后经过有氧呼吸、反硝化、锰铁氧化物还原、硫酸盐还原和CO_2还原等过程[3],构成沉积物剖面上理想的氧化还原序列(图1)[4]。当甲烷生成后,可以向上扩散,与孔隙水中的硫酸盐发生甲烷厌氧氧化(AOM)反应,并且在硫酸盐—甲烷转换带内(SMTZ)生成大量硫化氢(H_2S)。另外,甲烷还可以直接和铁锰氧化物反应,例如甲烷厌氧氧化—铁还原过程[5]。上述有机质矿化过程中,硫酸盐还原是边缘海沉积物内有机质矿化最主要的途径,并且大约70%的硫酸盐还原发生在大陆架沉积环境,占沿岸沉积物有机质矿化的一半以上[2,6]。海水硫酸盐经过微生物硫酸盐还原(MSR)产生H_2S,随后与活性铁反应形成铁硫化物而埋藏在海洋沉积物中[7-8]。自生黄铁矿(FeS_2)是海洋沉积物中硫化物最主要的矿物形态[9],其形成过程伴随着有机质矿化,硫酸盐还原以及铁氧化物的还原等成岩过程,是研究海洋沉积物内C-S-Fe生物地球化学循环的重要载体[10-12]。黄铁矿形成的成岩环境和成岩路径可以通过其形貌、粒径[10,13-15]、铁同位素[16]以及硫同位素[17-21]等指标进行示踪,因此,以自生黄铁矿为载体,可以利用多种指标研究边缘海沉积物内黄铁矿的形成机制及硫同位素组成。但是,在现实环境中,由于沉积物经常受到再悬浮,生物扰动、事件沉积等因素的影响,往往导致氧化还原带的相互重叠或者缺失[22],形成非稳态的沉积成岩环境[23-24]。因此,沉积环境在黄铁矿的

收稿日期:2019-07-08; **收修改稿日期**:2019-08-06

基金项目:国家自然科学基金项目(41976053,41430965,41606062);"科学"高端用户项目(KEXUE2017G15)[**Foundation**: National Natural Science Foundation of China, No. 41976053, 41430965, 41606062; Senior User Project of RV KEXUE, No. KEXUE2017G15]

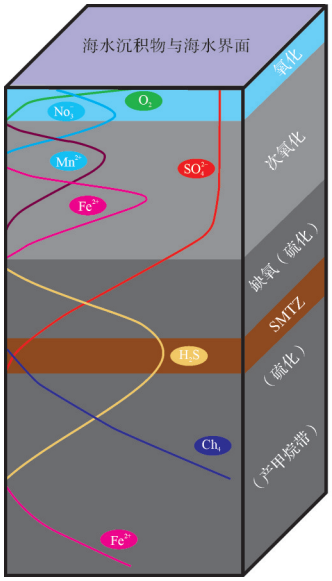

有氧氧化：
$(CH_2O)106(NH_3)16(H_3PO_4)+138O_2$
$\rightarrow 106CO_2+16HNO_3+H_3PO_4+122H_2O$
反硝化：
$(CH_2O)106(NH_3)16(H_3PO_4)+84.8HNO_3$
$\rightarrow H_3PO_4+148.4H_2O+106CO_2+42.4N_2+16NH_3$
锰还原：
$(CH_2O)106(NH_3)16(H_3PO_4)+472H^++236MnO_2$
$\rightarrow H_3PO_4+106CO_2+236Mn^{2+}+8N2+366H_2O$
铁还原：
$(CH_2O)106(NH_3)16(H_3PO_4)+424FeOOH+848H^+$
$\rightarrow 424Fe^{2+}+106CO_2+16NH_3+H_3PO_4+742H_2O$
有机质硫酸盐还原：
$(CH_2O)106(NH_3)16(H_3PO_4)+53SO_4^{2-}$
$\rightarrow H_3PO_4+106H_2O+106CO_2+16NH_3+53S^{2-}$
甲烷厌氧氧化—硫酸盐还原：
$CH_4+SO_4^{2-}\rightarrow HCO_3^-+HS^-+H_2O$
甲烷产生：
$(CH_2O)106(NH_3)16(H_3PO_4)$
$\rightarrow H_3PO_4+53CO_2+53CH_4+16NH_3$
甲烷厌氧氧化—铁还原：
$CH_4+8Fe(OH)_3+15H^+\rightarrow HCO_3^-+8Fe^{2+}+21H_2O$
SMTZ: sulfate-methane transition zone (硫酸盐—甲烷转换带)

图1　理想的稳定状态下有机质矿化及其形成的氧化还原带（修改自文献[4]）
有机质矿化反应序列依据文献[3]，甲烷厌氧氧化—铁还原反应依据文献[5]
Fig.1　Organic mineralization and steady-state redox zones（modified from reference[4]）

形成过程及其同位素组成方面也起到非常重要的作用，本文重点论述局部沉积环境的改变对沉积物内无机硫生物地球化学循环的影响，希望可为研究自生黄铁矿相关的早期成岩及生物地球化学过程起到抛砖引玉的效果。

1　全球硫循环及硫同位素组成

全球硫生物地球化学循环过程伴随着多种微生物新陈代谢过程（例如，硫酸盐还原、歧化反应和硫化物氧化等），影响全球长时间尺度的碳循环、气候演化以及氧气含量[25-27]。海洋作为全球最大的硫储库，其海水硫酸盐硫同位素值约为21‰[28]，其同位素组成主要受到通过河流输入的来自大陆风化产物的控制；另外火山喷发和洋中脊的玄武岩脱气过程也有所贡献，但是通量较小（图2）[25]。风化产物中的硫酸盐包括蒸发岩的溶解，碳酸盐岩的风化以及硫化物的氧化等，由于地壳中硫化物的同位素值比较低，并且丰度大于蒸发岩，因此河流输入硫酸盐的同位素值比海水要低很多，大约在5‰左右[29]。硫酸盐埋藏进入海洋沉积物的形式包括蒸发岩、碳酸盐岩和黄铁矿，其中进入碳酸盐矿物晶格的硫比较少（图2）。蒸发岩在地质历史中曾经是重要的汇[30]，但现代海洋中黄铁矿是最重要的汇[25]。根据物质守恒原理，海水硫酸盐的硫同位素主要与河流输入硫酸盐硫同位素（$\delta^{34}S_{输入}$），黄铁矿埋藏（$f_{黄铁矿}$）和MSR导致的硫同位素分馏有关（ε_{MSR}），因此搞清楚黄铁矿形成过程中的硫同位素分馏对理解全球硫循环及其在地质历史中的演化至关重要[31-34]。

$$\delta^{34}S_{海水硫酸盐}=\delta^{34}S_{输入}+f_{黄铁矿}\times\varepsilon_{MSR} \quad (1)$$

2　硫酸盐还原及硫同位素分馏

2.1　微生物硫酸盐还原（MSR）

自生黄铁矿根据其形成的环境可以分为同生黄铁矿（海水中形成的）和成岩黄铁矿（沉积物孔隙水形成的）[35]，最近的研究结果表明自生黄铁矿可以在短时间内生成，并且同生阶段比早期成岩阶段的莓状黄铁矿粒度要小[36]。有机质通过MSR，产生H_2S（反应见图1），其中一部分被重新氧化[6]，另一部分与铁氧化物反应，结合成单硫化合物（FeS），经过不同的成岩路径最终生成黄铁矿[7,9,35,37]。

在硫酸盐还原过程中，微生物首先利用$^{32}SO_4^{2-}$，伴随着相关的硫歧化反应[38]，所以其产生的H_2S相对于海水SO_4^{2-}亏损^{34}S，因此MSR是硫同位素分馏的主要机制。生成的H_2S与活性铁结合成铁硫化合物的过程以及最终黄铁矿的沉淀过程中同位素分馏可以忽略不计，所以黄铁矿硫同位素值可以代表H_2S的硫同位素值，产生的黄铁矿硫同位素表现出亏损^{34}S的特征[39]。之前的研究认为大于46‰的分馏必须伴随

着硫歧化反应[27,38]，但近些年的室内培养和实验模拟研究表明，单纯的硫酸盐还原过程（不需要歧化反应）也可以产生高达70‰的分馏[40-42]。

MSR过程中硫同位素的分馏主要受到微生物群落、硫酸盐还原速率和成岩系统开放程度的影响[43]。室内实验的结果表明硫同位素分馏程度与MSR的反应速率成反比，即硫酸盐还原速率越快，生成的H_2S同位素值越接近海水SO_4^{2-}的硫同位素值，富含^{34}S[44]。在开放体系中，孔隙水中的SO_4^{2-}不断得到上覆海水的补充，孔隙水中的SO_4^{2-}的硫同位素值基本保持不变，从而产生亏损^{34}S的H_2S，同位素分馏较大（图3a）[45]；与之相反，相对封闭的成岩系统内，SO_4^{2-}浓度得不到上覆海水的及时补充，随着反应的进行，孔隙水中会富集硫同位素较重的SO_4^{2-}（图3b）[45]。虽然MSR过程中的生物分馏（ε_{MSR}）保持不变，但由于瑞利分馏效应，使得自生黄铁矿的$\delta^{34}S$值接近孔隙水中的SO_4^{2-}的$\delta^{34}S$值[46]，表现出来的同位素分馏（$\Delta^{34}S$）较小[47]。

除了有机质的硫酸盐还原外，甲烷厌氧氧化（AOM）也能够强烈影响硫酸盐还原过程（反应见图1），此时，甲烷替代有机碳成为消耗硫酸盐的主要途径[1,48-50]。AOM过程不仅影响沉积物内硫化物的含量，也影响其硫同位素组成[51-53]，通常会导致自生黄铁矿富集^{34}S，经常用来指示SMTZ的位置[54-55]。但是水合物背景下产生的自生黄铁矿不一定富集^{34}S，例如南海北部神狐海域浅表层沉积物柱状样Site 4B中自生黄铁矿的硫同位素值（$\delta^{34}S$）介于−41.69‰~−49.16‰[56]。最近Feng *et al.*[57]等对已发表的南海天然气水合物背景下自生黄铁矿硫同位素值（包括沉积物内获取的还原态硫，显微镜下手工挑选的黄铁矿，以及原位测试的黄铁矿同位素）进行统计，发现硫同位素组成跨度很大（−51.3‰~114.8‰），与黄铁矿的具体成岩过程和生成阶段有关。利用二次离子质谱（SIMS）对自生黄铁矿进行原位硫同位素的研究能够区分不同生长阶段的黄铁矿硫同位素分馏特

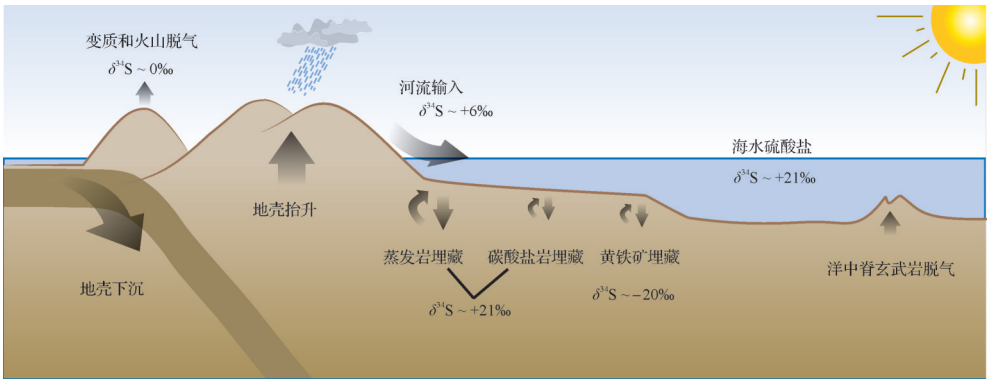

图2 全球硫循环及其同位素组成（修改自文献[25]）

Fig.2 Global sulfur cycle and its isotopic composition (modified from reference [25])

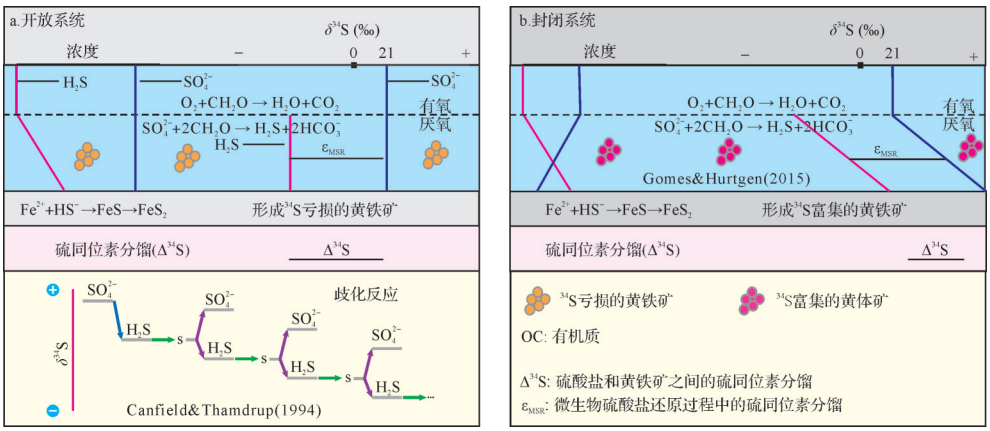

图3 成岩系统的开放性对硫酸盐还原过程中硫同位素的影响（修改自文献[45]）

（a）开放系统，一般形成^{34}S亏损的黄铁矿，此时可能伴随着硫的歧化反应；（b）封闭系统，随着硫酸盐还原反应的进行，自生黄铁矿会富集^{34}S，尽管生物分馏（ε_{MSR}）保持不变，但表现出来的同位素分馏（$\Delta^{34}S$）却变小

Fig.3 Effect of openness of diagenetic systems on sulfur isotope (modified from reference [45])

征，进而恢复其形成的成岩路径[53,58]。利用^{35}S放射性示踪的实验也证明在SMTZ内，有机质与甲烷硫酸盐还原同时进行，与AOM过程同时消耗孔隙水中的硫酸盐[59-60]。

2.2　非稳态环境中黄铁矿的硫同位素

在浅水沉积环境中，表层沉积物往往受到波浪、海流和潮流等物理过程和生物扰动等生物过程的再改造，形成移动的泥质层（mobile mud），例如，现代亚马逊泥质区[61]和东海浙闽沿岸泥质区[62]。这些泥质层的厚度取决于陆源物质输入，潮流，上升流，以及季风和台风等因素，其沉积和随后的再悬浮影响沉积有机物质的再矿化过程[63]。移动泥质层含水量高，具有高度流动性，再悬浮过程导致沉积物强烈混合，加深了O_2，NO_3^-，Mn^{4+}和Fe^{3+}等氧化过程的深度，破坏了稳定状态下的氧化还原序列，混合了先前分层的同位素信号，形成非稳态成岩环境（图4a，b）[64]。在非稳态成岩环境中，移动泥质层中以铁锰氧化物还原为主，下伏地层产生的H_2S扩散到表层沉积物后被重新氧化，造成残留的H_2S富含^{34}S[65]，并且影响孔隙水中硫酸盐的硫同位素组成[66]。随后当氧气被消耗时（图4a）[64]，在有机质矿化的铁还原阶段，产生的活性铁与这种富含^{34}S的H_2S反应形成富含^{34}S的黄铁矿[25]。这可能会导致地球化学记录保留硫酸盐和硫化物之间的同位素分馏（$\Delta^{34}S$）变小甚至变负值，但并不代表微生物硫酸盐还原过程中的同位素分馏（ε_{MSR}）的减小[24,67]。

相对于深水环境，浅水沉积环境中，沉积物再改造、沉积速率、活性铁和有机质的增加有利于发展为封闭的成岩环境[11]。在封闭环境中，硫酸盐被微生物消耗的速度快于从上覆水柱补充的硫酸盐，因此随着渐进式MSR的发生，孔隙水硫酸盐和生成H_2S的硫同位素值平行增加（图4c）[11]，形成富含^{34}S的黄铁矿[68]。上述过程以及生物扰动可以导致在短的空间和时间尺度上产生极大地波动，而在深水环境中，沉积环境相对稳定，而较低的沉积速率使孔隙水与海水的交换通畅，这可能导致较低且比较稳定的黄铁

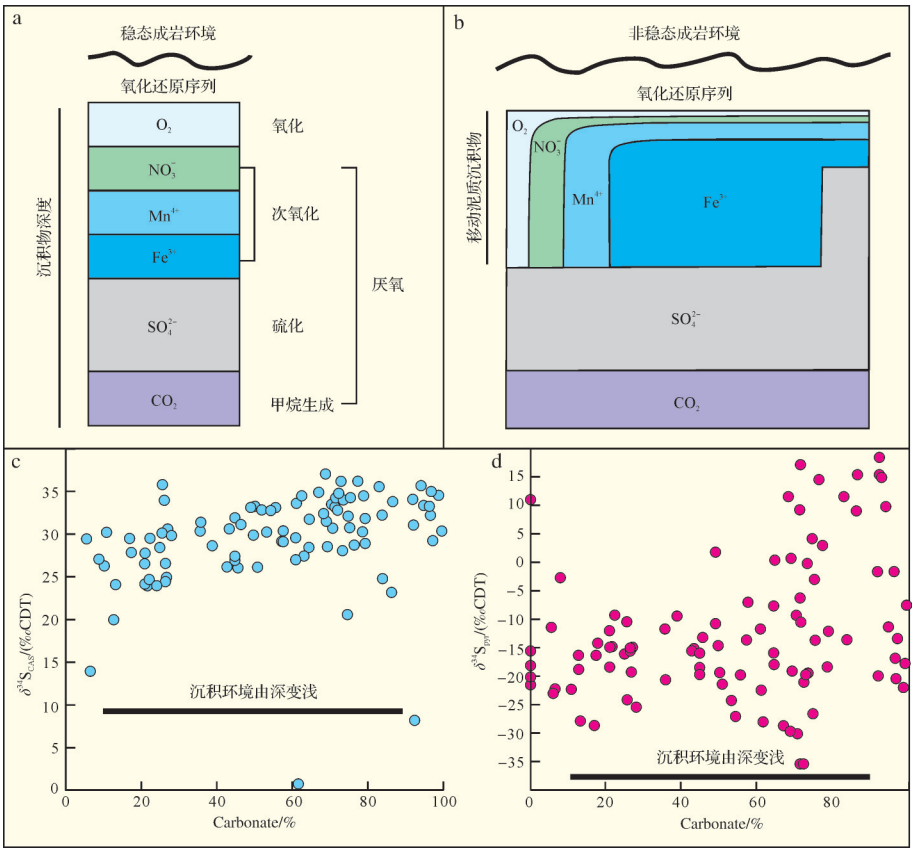

图4　不同成岩环境中的氧化还原序列和硫同位素组成

（a）（b）稳定和非稳定状态的氧化还原序列，修改自文献[64]；（c）（d）浅水沉积环境中，硫同位素受到沉积环境的控制。注意浅水环境中黄铁矿硫同位素值分布范围非常广泛，碳酸盐岩（Carbonate）含量代表不同的沉积环境，含量越多代表水深越浅，修改自文献[11]

Fig.4　Redox sequence and sulfur isotope composition in different diagenetic environments

矿硫同位素值(图4d)[11]。因此,在利用黄铁矿硫同位素指示深时古海洋演化的研究中,要特别注意黄铁矿形成的沉积环境,尤其是浅水环境中的黄铁矿硫同位素值要做慎重的评价[25]。

3 沉积速率对黄铁矿硫同位素的影响

在海洋沉积环境中,沉积模式和沉积速率受控于冰期—间冰期旋回引起的海平面和气候变化[69],进而可能影响MSR过程中黄铁矿的形成及其硫同位素组成[70-71]。

3.1 沉积速率对成岩系统开放性的影响

Pasquier *et al.*[68]对地中海300 m钻孔岩芯沉积物(钻孔PRGL1-4,图5a)的研究表明黄铁矿$\delta^{34}S_{pyr}$值在冰期和间冰期存在明显的区别:冰期黄铁矿硫同位素具有高$\delta^{34}S$值和高变异性(平均$\delta^{34}S=-15.2‰\pm9.0‰$,$n$=46);而间冰期具有低$\delta^{34}S$值和变异性的特征(平均$\delta^{34}S=-41.6‰\pm2.2‰$,$n$=19;图5b)。在同一钻孔获得的有孔虫氧同位素数据表明,岩芯连续记录了50万年以来最后五个冰期—间冰期旋回的历史(图5c),其时间跨度远远短于海相硫酸盐的停留时间,因此黄铁矿中保存的硫同位素值($\delta^{34}S_{pyr}$)记录的任何变化必然对应于其形成环境的变化[68]。该钻孔沉积物黄铁矿硫同位素介于-44.0‰和32.3‰,波动大于76‰,与冰期间冰期旋回引起的海平面变化有良好的对应关系(图5c)。具体来说,冰期海平面降低,陆源碎屑物质更容易搬运到钻孔位置,因此沉积速率增加,沉积物容易受到短期随机变化的影响条件,包括沉积物特征(有机质输入,沉积速率,物理扰动等)和底栖生态学(生物扰动,微生物席等),进而影响黄铁矿的形成和最终的硫同位素组成[25],即前文所提到的非稳态成岩环境。与之相反,在间冰期,海平面升高,海岸线后退,陆源输入速率降低,沉积速率变慢,形成相对稳定的沉积环境,黄铁矿硫同位素

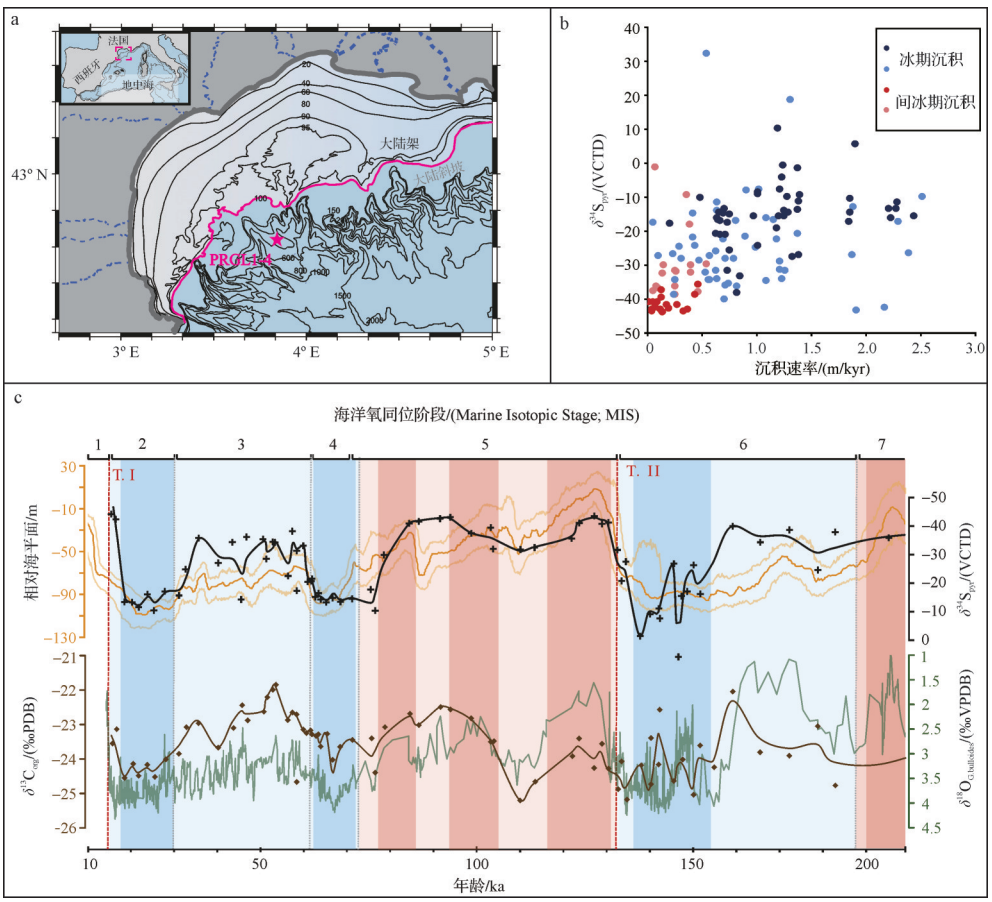

图5 黄铁矿硫同位素组成与海平面变化之间的关系(修改自文献[68])

(a)钻孔PRGL1-4在地中海的位置;(b)沉积速率对黄铁矿硫同位素的影响,注意冰期和间冰期沉积速率的差异;(c)200 ka以来黄铁矿硫同位素信号与海平面变化具有良好的对应关系;浅蓝色代表冰期,深蓝色代表代表严格意义上的冷期(低海平面,高沉积速率);浅橙色代表间冰期,深橙色代表严格意义上的暖期(高海平面,低沉积速率)

Fig.5 Relationship between sulfur isotope composition and sea-level change (modified from reference [68])

值降低且相对稳定（图5c）。上述结果表明沉积过程对硫同位素记录的影响（通过影响孔隙水和上覆海水的连通性），特别是沉积环境与海平面变化有关的区域，并表明可以从黄铁矿$\delta^{34}S$记录中得出有意义的古环境信息[68]。上述研究中，作者还提出沉积速率随海平面变化引起有机质输入的改变，进而可以影响硫酸盐还原速率，并最终记录在硫同位素信号中，但海洋沉积物中硫酸盐还原速率普遍较低[26]，说明成岩系统的开放程度是主要因素。近年来，局部沉积环境对硫同位素影响的研究已经延伸到古生代的黄铁矿和硫酸盐硫同位素的解释[25,72]，其重要性已经得到国内外同行的重视[10,66-67]，对理解深时古海洋演化及地球系统演化具有重要启示意义。

3.2　沉积速率影响氧化还原带的迁移

沉积速率的改变不仅能影响成岩系统的性质，还能引起氧化还原带的迁移，例如沉积速率的改变导致硫酸盐—甲烷转化带（SMTZ）的迁移，进而影响硫化物的组成及其同位素特征：冰期/间冰期转换引起的沉积速率突然下降，导致沉积柱中SMTZ在某一深度停滞较长时间，铁的氢氧化物、氧化物大量溶解，而富^{34}S的自生黄铁矿明显积累[24,73]。上述结果表明沉积速率可以通过改变成岩系统的开放性（瑞利分馏）和SMTZ的迁移（通过AOM）影响黄铁矿硫同位素，但具体哪种机制起主导作用还需要结合地质背景并利用多种指标进行约束。Hilligsøe *et al.*[74]结合地震声学调查和沉积物岩芯的地球化学分析，探讨了波罗的海南部博恩霍尔姆盆地（Bornholm Basin）泥质沉积物中甲烷通量的分布（图6）。该研究首先利用地球物理测绘全新世泥质沉积厚度（富含有机质；图6a）以及全新世沉积物中捕获的甲烷气泡上界的深度分布，然后将这两个参数与来自44个站点的沉积物孔隙水地球化学数据对比，发现甲烷的产生与通量及硫酸盐的消耗与沉积物厚度相关（图6a，b），说明沉积厚度（沉积速率）直接控制了甲烷的产生及其在海洋沉积物中的扩散，决定了SMTZ的深度。

在缺乏孔隙水数据的情况下，氧化还原带的转化经常通过环境磁学的方法进行示踪，其中最主要的依据就是不同形态的含铁矿物磁学性质的差异[75-77]，并在中国东海内陆架泥质区内取得了良好应用[78-80]。在东海内陆架泥质区内，主要的磁性矿物是磁铁矿，随着深度的加深和早期成岩过程，磁化率分两步降低：第一次发生在0.15~1.1 m的深度，可能指示硫酸盐还原带的深度；第二次磁性信号的减弱发生在3.2~5.8 m，并包含两个具有极低磁性矿物质含量的沉积层分别对应于现在和之前SMTZ的位置[81]。因此，环境磁学为研究早期成岩过程中氧化还原的分带提供了重要参考，在古代地层记录（没有孔隙水数据）的研究中显得尤为重要[82]。

4　东海内陆架泥质区内自生黄铁矿硫同位素的沉积约束

作为世界上最为宽广的陆架之一，东海内陆架沉积过程受到大陆和岛屿河流的显著影响（例如长江、黄河、台湾河流；图7a）[80]，其陆源碎屑沉积物和有机质输入丰富，沉积速率高，是研究全新世古气候和古海洋演化的绝佳场所[85-87]。东海陆架底质沉积

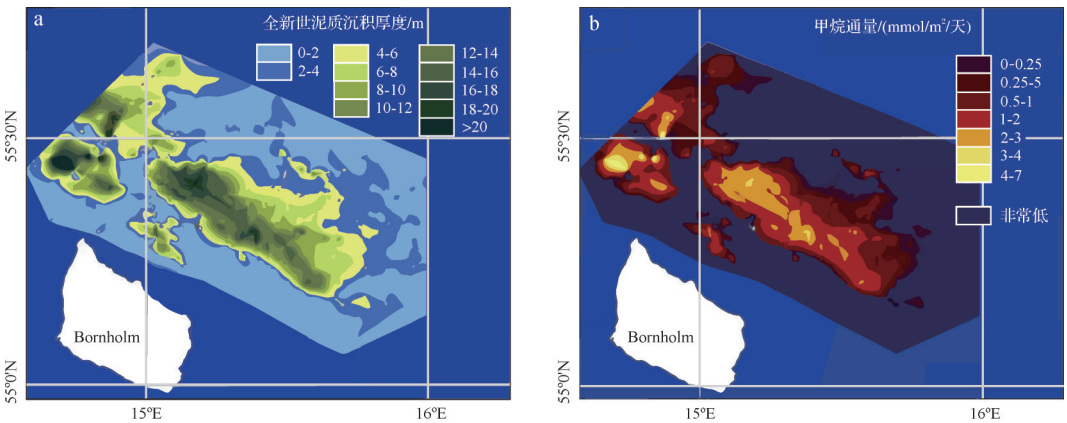

图6　博恩霍尔姆盆地泥质沉积层厚度与硫酸盐甲烷转换带位置对比（修改自文献[74]）

（a）全新世泥沉积层的厚度（m）；（b）甲烷通量，代表SMTZ的位置

Fig.6　Relationship between thickness of marine Holocene mud and methane flux in the Bornholm Basin, Baltic Sea（modified from reference [74]）

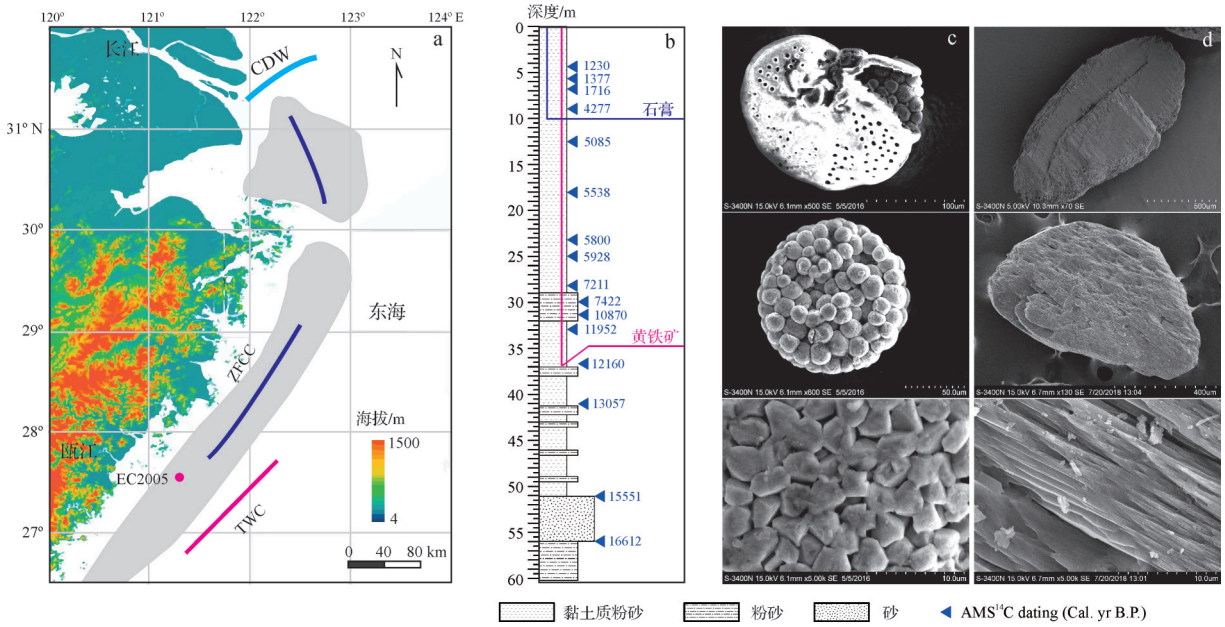

图7 东海内陆架泥质沉积区域背景和洋流系统以及部分自生黄铁矿和石膏扫描电镜图片

(a)东海接收长江、浙闽和台湾河流的陆源物质,主要洋流系统包括ZFCC:浙闽沿岸流;TWC:台湾暖流;KC:黑潮,据文献[80];(b)EC2005钻孔(121.33° E,27.42° N)位于水深36 m的浙闽泥质沉积中心,岩芯长度达到60 m(17.3 ka),据文献[83];(c)自生黄铁矿集合体呈现球状、棒状和块状等形貌,并发育溶蚀孔,据文献[45];(d)钻孔沉积物最上部10 m发现自生石膏,是硫化物再氧化的结果,据文献[84]

Fig.7 Regional background and ocean current system in the East China Sea and representative scanning electron micrographs of authigenic pyrite and gypsum

物类型分布的基本格局是在砂质沉积的背景上分布着大范围的泥质沉积[88]。全新世高水位期以来(7.5 ka),输入东海的细粒陆源沉积物在洋流、地形等因素的控制作用下,形成了东海外陆架的济州岛西南泥质区、长江口泥质区以及位于东海内陆架的浙闽沿岸泥质区[89-91]。因此,东海内陆架泥质区的沉积环境演化受到东亚季风变化、洋流分布、以及沉积动力过程的控制[92-94],其沉积速率在时空分布上呈现出较大的波动[95]。末次冰消期以来东海内陆架经历了快速的海侵过程,其沉积环境发生明显改变,从陆相环境过渡到海相环境[83,96-97]。上述沉积环境巨变引起沉积物和有机质来源的转变,活性铁和硫酸盐供给的波动,SMTZ的迁移,必将影响到自生黄铁矿的形成以及硫同位素组成,为研究非稳态环境下硫循环提供了契机[45,84]。

前人对东海内陆架沉积物开展的自生黄铁矿相关研究主要集中在自生黄铁矿的形貌特征及其形成的控制因素上[98]。例如,Duan *et al.*[99]根据沉积物孔隙水的研究,指出不同的沉积环境和硫来源导致自生黄铁矿具有不同的形貌和硫同位素特征。由于较低的活性有机质含量和非稳态的沉积环境,东海沉积物自生黄铁矿含量很低,其形成与保存与有机质的埋藏速率有关[100-101]。由于东海内陆架接收大量富含铁的细粒陆源沉积物,泥质沉积区内活性铁含量很高,因此沉积物内硫酸盐过程可能受到异化铁还原的抑制[102]。环境磁学的研究结果表明东海内陆架泥质区硫酸盐还原的深度和磁性矿物的性质受到沉积速率的控制[80-81,103],并且可能受到生物成因甲烷气的影响[79]。

浅表层自生黄铁矿硫同位素的结果表明东海陆架泥质区内自生黄铁矿硫同位素值偏轻,同位素分馏受到硫酸盐还原和歧化反应的影响[63]。最近,对EC2005钻孔(60 m)的研究结果表明:自生黄铁矿大量出现在40 m以浅的沉积物内表现出不同的晶体组合类型,以莓状黄铁矿为主(图7b,c)。因为在东海内陆架泥质区,黄铁矿硫是还原态硫的主要赋存形式[104],所以利用镉还原法[105]提取自生黄铁矿硫,并测试其硫同位素值。我们最新的研究结果表明16.5 ka以来自生黄铁矿硫同位素δ^{34}S值的变化范围为−38.2‰至15.0‰,变化区间达到53.2‰(图8)[45]。在12.3 ka之前的淡水沉积沉积环境,黄铁矿丰度很低,并且其δ^{34}S值位于典型淡水环境的范围内(8a,b)[45]。在12.3 ka之后,海平面到达研究区,黄铁矿δ^{34}S值与沉积速率(r=0.78,p<0.01)显著相关[45]。具

体而言,低沉积速率倾向于形成开放的成岩系统,持续的海水供应可防止孔隙水硫酸盐因为MSR反应的进行而变得富含^{34}S,因此生成的黄铁矿同位素值偏轻(富集^{32}S;图8c,d)[45]。与之相反,高沉积速率有利于形成相对封闭的成岩系统,孔隙水中的硫酸盐随着MSR的进行而得不到有效补充,进而孔隙水硫酸盐富集^{34}S,所以形成的黄铁矿也富集^{34}S,掩盖了微生物硫酸盐过程中生物分馏(ε_{MSR})的程度(图3)。上述研究成果表明自生黄铁矿的硫同位素组成,受到沉积速率的影响,特别是在非稳态沉积环境内,因此在解释地层记录中黄铁矿硫同位素信号时要特别注意其沉积背景和沉积环境的演化[66]。

此外,在EC2005岩芯最上部的十米出现自生石膏,呈现出典型的石膏晶体形貌(图7d)[84],在相同层位也同时发育大量自生黄铁矿,并且在某些层位的自生黄铁矿晶体表面出现溶蚀坑(图7c)[45],该类型的溶蚀孔很有可能是自生黄铁矿氧化的结果[106]。同位素测试的结果表明,自生石膏的硫同位素明显富集^{32}S,代表其来源于MSR的自生黄铁矿,通过端元计算,显示大约70%的硫源自于自生黄铁矿[84],该过程可能与上文中提到的在非稳态环境中氧化还原带的迁移有关。石膏氧同位素的结果也是明显负偏,证明该自生石膏是原位生成的,不是在后期沉积物保存过程中形成的,而是形成在沉积物氧化还原带的铁、锰氧化带内[107]。东海内陆的研究结果表明,在非稳态沉积环境内,除了有机质矿化(MSR),沉积过程在沉积物C-S-Fe循环中也扮演着重要角色,需要进一步的研究。

5　总结与展望

边缘海沉积物中的自生黄铁矿是还原态硫的主要载体,其形成过程与硫循环和有机质矿化密切相关,直接影响全球C-S-Fe生物地球化学循环[2]。自生黄铁矿的形成过程和硫同位素组成除了受到MSR过程的控制之外还受到边缘海沉积环境的影响[25],例如在海侵之前的淡水环境和海侵之后的海洋环境具有不同的成岩路径[108],海平面和气候变化引起的成岩系统开放性的差异等[68]。

末次冰消期以来,全球海平面上升导致东海内陆架由陆相环境过渡到海相环境,并在全新世高海平面时期发育东海内陆架泥质沉积[109]。近十几年来,国内外学者在东海内陆架开展了一系列沉积物源—汇过程和环境响应的研究,相对而言,东海内陆架沉积物硫循环过程的研究还很薄弱。初步研究表明,东海内陆架泥质区为研究沉积物内硫循环及相关科学问题提供了绝佳的条件,有望在如下方面取

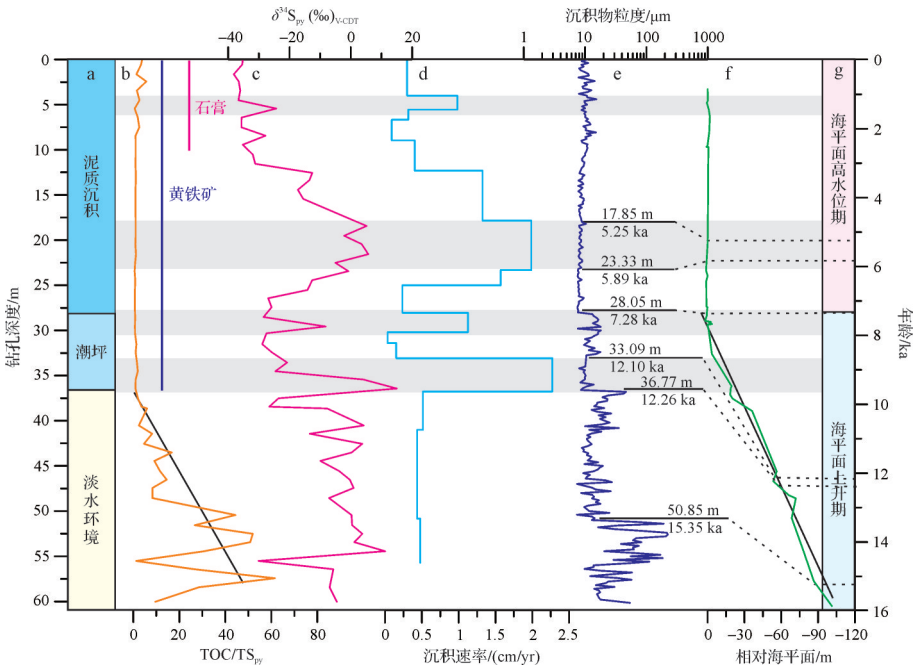

图8　东海内陆架泥质区EC2005钻孔自生黄铁矿硫同位素和沉积环境(修改自文献[45])

Fig.8　Sulfur isotopes of pyrite from core EC2005, and the sedimentary environment of the mud area of the East China Sea (modified from reference [45])

得开创性成果。

（1）沉积环境对自生黄铁矿硫同位素的约束机制。尽管已有的研究表明非稳态环境中，有利于成岩系统向封闭系统演化，进而形成富含^{34}S的黄铁矿，但高的沉积速率可能导致有机质的快速供应并有利于有机质保存，从而提高MSR的反应速率，减少同位素分馏，形成富含^{34}S的黄铁矿。上述机制的区分，除了需要孔隙水的数据支撑外，原位硫同位素的测试或许具有更重要的意义，毕竟在地层记录中很难取得孔隙水数据[110]。

（2）异化铁还原和硫酸盐还原之间的关系。浅表层沉积物的研究表明异化铁还原可能在中国东部边缘海有机质矿化过程中起到非常重要的作用[111]，但EC2005钻孔的研究表明硫酸盐还原过程也起着重要作用[45]。因此怎样区分异化铁还原和硫酸盐还原过程在黄铁矿形成中的作用显得非常必要，铁同位素的研究或许会提供一些思路[49,112]。

（3）SMTZ内除了AOM阻止温室气体甲烷扩散到大气中之外[60]，硫酸盐还被有机质还原，怎样区分AOM与有机质对硫酸盐还原的贡献是研究现代海洋硫循环的热点和难点[59]。东海内陆架泥质沉积物内有生物成因甲烷气的产生[113]，为研究上述科学问题提供了难得的材料，值得进一步开展研究，特别是沉积物孔隙水地球化学和多硫同位素的研究。

（4）SMTZ上下层位内铁还原相关的甲烷厌氧氧化（Fe-AOM）日益受到关注，是消耗甲烷的重要途径，并导致含铁自生矿物的形成[114-115]。东海内陆架在末次冰盛期为陆相沉积环境，随着末次冰消期海平面升高转化为海相沉积环境，会不会在全新世泥质沉积物下伏地层中产生甲烷，以及泥质区内形成的硫化物能否扩散到下伏地层中，导致形成新的自生矿物，都值得开展深入研究。

致谢 论文的撰写过程得到美国华盛顿大学David Fike教授的指导，评审专家为本文提供了宝贵的修改建议，在此表示感谢。并感谢中国地质大学（武汉）陈中强教授和编辑部对本专栏的组织。

参考文献（References）

[1] 吴自军，任德章，周怀阳. 海洋沉积物甲烷厌氧氧化作用（AOM）及其对无机硫循环的影响[J]. 地球科学进展，2013，28（7）：765-773.［Wu Zijun，Ren Dezhang，Zhou Huaiyang. Anaerobic Oxidation of Methane（AOM）and its influence on inorganic sulfur cycle in marine sediments[J]. Advances in Earth Science，2013，28（7）：765-773.］

[2] Jørgensen B B，Kasten S. Sulfur cycling and methane oxidation[M]//Schulz H D，Zabel M. Marine geochemistry. Berlin，Heidelberg：Springer，2006：271-309.

[3] Froelich P N，Klinkhammer G P，Bender M L，et al. Early oxidation of organic matter in pelagic sediments of the eastern equatorial Atlantic：suboxic diagenesis[J]. Geochimica et Cosmochimica Acta，1979，43（7）：1075-1090.

[4] Egger M J. Anaerobic oxidation of methane and its impact on iron and phosphorus cycling in marine sediments[D]. Utrecht：University Utrecht，2016.

[5] Beal E J，House C H，Orphan V J. Manganese- and iron-dependent marine methane oxidation[J]. Science，2009，325（5937）：184-187.

[6] Jørgensen B B. Mineralization of organic matter in the sea bed—the role of sulphate reduction[J]. Nature，1982，296（5858）：643-645.

[7] Berner R A. Sedimentary pyrite formation：An update[J]. Geochimica et Cosmochimica Acta，1984，48（4）：605-615.

[8] Raiswell R，Hardisty D S，Lyons T W，et al. The iron paleoredox proxies：A guide to the pitfalls，problems and proper practice[J]. American Journal of Science，2018，318（5）：491-526.

[9] Raiswell R，Canfield D E. The iron biogeochemical cycle past and present[J]. Geochemical Perspectives，2012，1（1）：1-220.

[10] Rickard D. Sedimentary pyrite framboid size-frequency distributions：A meta-analysis[J]. Palaeogeography，Palaeoclimatology，Palaeoecology，2019，522：62-75.

[11] Richardson J A，Keating C，Lepland A，et al. Silurian records of carbon and sulfur cycling from Estonia：The importance of depositional environment on isotopic trends[J]. Earth and Planetary Science Letters，2019，512：71-82.

[12] Maharjan D，Jiang G Q，Peng Y B，et al. Sulfur isotope change across the Early Mississippian K－O（Kinderhookian－Osagean）$\delta^{13}C$ excursion[J]. Earth and Planetary Science Letters，2018，494：202-215.

[13] Wilkin R T，Arthur M A. Variations in pyrite texture，sulfur isotope composition，and iron systematics in the Black Sea：Evidence for Late Pleistocene to Holocene excursions of the O_2-H_2S redox transition[J]. Geochimica et Cosmochimica Acta，2001，65（9）：1399-1416.

[14] Wilkin R T，Barnes H L，Brantley S L. The size distribution of framboidal pyrite in modern sediments：An indicator of redox conditions[J]. Geochimica et Cosmochimica Acta，1996，60（20）：3897-3912.

[15] Huang Y G，Chen Z Q，Wignall P B，et al. Latest Permian to middle Triassic redox condition variations in ramp settings，South China：Pyrite framboid evidence[J]. Geological Society of America Bulletin，2017，129（1/2）：229-243.

[16] Lin Z Y，Sun X M，Lu Y，et al. The enrichment of heavy iron isotopes in authigenic pyrite as a possible indicator of sulfate-

driven anaerobic oxidation of methane: Insights from the South China Sea[J]. Chemical Geology, 2017, 449: 15-29.

[17] Antler G, Turchyn A V, Ono S, et al. Combined ^{34}S, ^{33}S and ^{18}O isotope fractionations record different intracellular steps of microbial sulfate reduction[J]. Geochimica et Cosmochimica Acta, 2017, 203: 364-380.

[18] Böttcher M E, Thamdrup B. Anaerobic sulfide oxidation and stable isotope fractionation associated with bacterial sulfur disproportionation in the presence of MnO_2[J]. Geochimica et Cosmochimica Acta, 2001, 65(10): 1573-1581.

[19] Canfield D E, Farquhar J, Zerkle A L. High isotope fractionations during sulfate reduction in a low-sulfate euxinic ocean analog[J]. Geology, 2010, 38(5): 415-418.

[20] Shi W, Li C, Luo G M, et al. Sulfur isotope evidence for transient marine-shelf oxidation during the Ediacaran Shuram Excursion[J]. Geology, 2018, 46(3): 267-270.

[21] Ma Z X, Liu X T, Yu W C, et al. Redox conditions and manganese metallogenesis in the Cryogenian Nanhua Basin: Insight from the basal Datangpo Formation of South China[J]. Palaeogeography, Palaeoclimatology, Palaeoecology, 2019, 529: 39-52.

[22] 朱茂旭,史晓宁,杨桂朋,等. 海洋沉积物中有机质早期成岩矿化路径及其相对贡献[J]. 地球科学进展,2011,26(4):355-364. [Zhu Maoxu, Shi Xiaoning, Yang Guipeng, et al. Relative contributions of various early diagenetic pathways to mineralization of organic matter in marine sediments: An overview [J]. Advances in Earth Science, 2011, 26(4): 355-364.]

[23] Aller R C, Madrid V, Chistoserdov A, et al. Unsteady diagenetic processes and sulfur biogeochemistry in tropical deltaic muds: Implications for oceanic isotope cycles and the sedimentary record[J]. Geochimica et Cosmochimica Acta, 2010, 74(16): 4671-4692.

[24] Riedinger N, Brunner B, Krastel S, et al. Sulfur cycling in an iron oxide-dominated, dynamic marine depositional system: The argentine continental margin[J]. Frontiers in Earth Science, 2017, 5: 33.

[25] Fike D A, Bradley A S, Rose C V. Rethinking the ancient sulfur cycle[J]. Annual Review of Earth and Planetary Sciences, 2015, 43: 593-622.

[26] Jørgensen B B, Findlay A J, Pellerin A. The biogeochemical sulfur cycle of marine sediments[J]. Frontiers in Microbiology, 2019, 10: 849.

[27] Canfield D E. Biogeochemistry of sulfur isotopes[J]. Reviews in Mineralogy and Geochemistry, 2001, 43(1): 607-636.

[28] Tostevin R, Turchyn A V, Farquhar J, et al. Multiple sulfur isotope constraints on the modern sulfur cycle[J]. Earth and Planetary Science Letters, 2014, 396: 14-21.

[29] Burke A, Present T M, Paris G, et al. Sulfur isotopes in rivers: Insights into global weathering budgets, pyrite oxidation, and the modern sulfur cycle[J]. Earth and Planetary Science Letters, 2018, 496: 168-177.

[30] Hurtgen M T. The marine sulfur cycle, revisited[J]. Science, 2012, 337(6092): 305-306.

[31] Canfield D E, Habicht K S, Thamdrup B. The Archean sulfur cycle and the early history of atmospheric oxygen[J]. Science, 2000, 288(5466): 658-661.

[32] Hurtgen M T, Arthur M A, Halverson G P. Neoproterozoic sulfur isotopes, the evolution of microbial sulfur species, and the burial efficiency of sulfide as sedimentary pyrite[J]. Geology, 2005, 33(1): 41-44.

[33] Fakhraee M, Hancisse O, Canfield D E, et al. Proterozoic seawater sulfate scarcity and the evolution of ocean - atmosphere chemistry[J]. Nature Geoscience, 2019, 12(5): 375-380.

[34] Turchyn A V, DePaolo D J. Seawater chemistry through Phanerozoic time[J]. Annual Review of Earth and Planetary Sciences, 2019, 47: 197-224.

[35] Raiswell R, Berner R A. Pyrite formation in euxinic and semi-euxinic sediments[J]. American Journal of Science, 1985, 285(8): 710-724.

[36] Rickard D. How long does it take a pyrite framboid to form?[J]. Earth and Planetary Science Letters, 2019, 513: 64-68.

[37] Berner R A. Sedimentary pyrite formation[J]. American Journal of Science, 1970, 268(1): 1-23.

[38] Canfield D E, Thamdrup B. The production of ^{34}S-depleted sulfide during bacterial disproportionation of elemental sulfur[J]. Science, 1994, 266(5193): 1973-1975.

[39] Gomes M L, Hurtgen M T. Sulfur isotope fractionation in modern euxinic systems: Implications for paleoenvironmental reconstructions of paired sulfate - sulfide isotope records[J]. Geochimica et Cosmochimica Acta, 2015, 157: 39-55.

[40] Brunner B, Bernasconi S M. A revised isotope fractionation model for dissimilatory sulfate reduction in sulfate reducing bacteria[J]. Geochimica et Cosmochimica Acta, 2005, 69(20): 4759-4771.

[41] Sim M S, Bosak T, Ono S. Large sulfur isotope fractionation does not require disproportionation[J]. Science, 2011, 333(6038): 74-77.

[42] Wortmann U G, Bernasconi S M, Böttcher M E. Hypersulfidic deep biosphere indicates extreme sulfur isotope fractionation during single-step microbial sulfate reduction[J]. Geology, 2001, 29(7): 647-650.

[43] Bradley A S, Leavitt W D, Schmidt M, et al. Patterns of sulfur isotope fractionation during microbial sulfate reduction[J]. Geobiology, 2016, 14(1): 91-101.

[44] Leavitt W D, Halevy I, Bradley A S, et al. Influence of sulfate reduction rates on the Phanerozoic sulfur isotope record[J]. Proceedings of the National Academy of Sciences of the United States of America, 2013, 110(28): 11244-11249.

[45] Liu X T, Fike D, Li A C, et al. Pyrite sulfur isotopes constrained by sedimentation rates: Evidence from sediments on the

East China Sea inner shelf since the late Pleistocene[J]. Chemical Geology, 2019, 505: 66-75.

[46] Gomes M L, Hurtgen M T. Sulfur isotope systematics of a euxinic, low-sulfate lake: Evaluating the importance of the reservoir effect in modern and ancient oceans[J]. Geology, 2013, 41(6): 663-666.

[47] Stebbins A, Algeo T J, Olsen C, et al. Sulfur-isotope evidence for recovery of seawater sulfate concentrations from a PTB minimum by the Smithian-Spathian transition[J]. Earth-Science Reviews, 2018, 195: 83-95.

[48] 张美,陆红锋,邬黛黛,等. 南海神狐海域自生黄铁矿分布、形貌特征及其对甲烷渗漏的指示[J]. 海洋地质与第四纪地质, 2017,37(6):178-188. [Zhang Mei, Lu Hongfeng, Wu Daidai, et al. Cross-section distribution and morphology of authigenic pyrite and their indication to methane seeps in Shenhu areas, South China Sea[J]. Marine Geology & Quaternary Geology, 2017, 37(6): 178-188.]

[49] 张现荣,孙治雷,魏合龙,等. 自生黄铁矿的微生物成矿机理及对冷泉泄漏的指示意义[J]. 海洋地质与第四纪地质,2017, 37(2):25-32. [Zhang Xianrong, Sun Zhilei, Wei Helong, et al. Micro-biomineralizaiton of authigenic pyrite and its implications for seafloor cold seeps[J]. Marine Geology & Quaternary Geology, 2017, 37(2): 25-32.]

[50] Wang M, Cai F, Li Q, et al. Characteristics of authigenic pyrite and its sulfur isotopes influenced by methane seep at Core A, Site 79 of the middle Okinawa Trough[J]. Science China Earth Sciences, 2015, 58(12): 2145-2153.

[51] Lin Q, Wang J S, Taladay K, et al. Coupled pyrite concentration and sulfur isotopic insight into the paleo sulfate-methane transition zone (SMTZ) in the northern South China Sea[J]. Journal of Asian Earth Sciences, 2016, 115: 547-556.

[52] Lin Q, Wang J S, Algeo T J, et al. Enhanced framboidal pyrite formation related to anaerobic oxidation of methane in the sulfate-methane transition zone of the northern South China Sea [J]. Marine Geology, 2016, 379: 100-108.

[53] Lin Z Y, Sun X M, Peckmann J, et al. How sulfate-driven anaerobic oxidation of methane affects the sulfur isotopic composition of pyrite: A SIMS study from the South China Sea[J]. Chemical Geology, 2016, 440: 26-41.

[54] Borowski W S, Rodriguez N M, Paull C K, et al. Are ^{34}S-enriched authigenic sulfide minerals a proxy for elevated methane flux and gas hydrates in the geologic record?[J]. Marine and Petroleum Geology, 2013, 43: 381-395.

[55] Jørgensen B B, Böttcher M E, Lüschen H, et al. Anaerobic methane oxidation and a deep H_2S sink generate isotopically heavy sulfides in Black Sea sediments[J]. Geochimica et Cosmochimica Acta, 2004, 68(9): 2095-2118.

[56] Xie L, Wang J S, Wu N Y, et al. Characteristics of authigenic pyrites in shallow core sediments in the Shenhu area of the northern South China Sea: Implications for a possible mud volcano environment[J]. Science China Earth Sciences, 2013, 56(4): 541-548.

[57] Feng D, Qiu J W, Hu Y, et al. Cold seep systems in the South China Sea: An overview[J]. Journal of Asian Earth Sciences, 2018, 168: 3-16.

[58] Bryant R N, Jones C, Raven M R, et al. Sulfur isotope analysis of microcrystalline iron sulfides using secondary ion mass spectrometry imaging: Extracting local paleo-environmental information from modern and ancient sediments[J]. Rapid Communications in Mass Spectrometry, 2019, 33(5): 491-502.

[59] Jørgensen B B, Beulig F, Egger M, et al. Organoclastic sulfate reduction in the sulfate-methane transition of marine sediments [J]. Geochimica et Cosmochimica Acta, 2019, 254: 231-245.

[60] Egger M, Riedinger N, Mogollón J M, et al. Global diffusive fluxes of methane in marine sediments[J]. Nature Geoscience, 2018, 11(6): 421-425.

[61] Aller R C. Mobile deltaic and continental shelf muds as suboxic, fluidized bed reactors[J]. Marine Chemistry, 1998, 61(3/4): 143-155.

[62] Wang J L, Du J Z, Baskaran M, et al. Mobile mud dynamics in the East China Sea elucidated using ^{210}Pb, ^{137}Cs, ^{7}Be, and ^{234}Th as tracers[J]. Journal of Geophysical Research: Oceans, 2016, 121(1): 224-239.

[63] Zhu M X, Chen K K, Yang G P, et al. Sulfur and iron diagenesis in temperate unsteady sediments of the East China Sea inner shelf and a comparison with tropical mobile mud belts (MMBs) [J]. Journal of Geophysical Research: Biogeosciences, 2016, 121(11): 2811-2828.

[64] Aller R C. Sedimentary diagenesis, depositional environments, and benthic fluxes[M]//Holland H D, Turekian K K. Treatise on geochemistry. 2nd ed. Amsterdam: Elsevier, 2014: 293-334.

[65] Fry B, Ruf W, Gest H, et al. Sulfur isotope effects associated with oxidation of sulfide by O_2 in aqueous solution[J]. Chemical Geology: Isotope Geoscience section, 1988, 73 (3): 205-210.

[66] Richardson J A, Newville M, Lanzirotti A, et al. Depositional and diagenetic constraints on the abundance and spatial variability of carbonate-associated sulfate [J]. Chemical Geology, 2019, 523: 59-72.

[67] Rose C V, Fischer W W, Finnegan S, et al. Records of carbon and sulfur cycling during the Silurian Ireviken Event in Gotland, Sweden[J]. Geochimica et Cosmochimica Acta, 2019, 246: 299-316.

[68] Pasquier V, Sansjofre P, Rabineau M, et al. Pyrite sulfur isotopes reveal glacial-interglacial environmental changes[J]. Proceedings of the National Academy of Sciences of the United States of America, 2017, 114(23): 5941-5945.

[69] Liu X T, Rendle-Bühring R, Meyer I, et al. Holocene shelf sedimentation patterns off equatorial East Africa constrained by

climatic and sea-level changes [J]. Sedimentary Geology, 2016, 331: 1-11.

[70] Claypool G E. Ventilation of marine sediments indicated by depth profiles of pore water sulfate and $\delta^{34}S$[J]. The Geochemical Society Special Publications, 2004, 9: 59-65.

[71] Chang L, Bolton C T, Dekkers M J, et al. Asian monsoon modulation of nonsteady state diagenesis in hemipelagic marine sediments offshore of Japan[J]. Geochemistry, Geophysics, Geosystems, 2016, 17(11): 4383-4398.

[72] Jones D S, Fike D A. Dynamic sulfur and carbon cycling through the end-Ordovician extinction revealed by paired sulfate - pyrite $\delta^{34}S$[J]. Earth and Planetary Science Letters, 2013, 363: 144-155.

[73] Riedinger N, Pfeifer K, Kasten S, et al. Diagenetic alteration of magnetic signals by anaerobic oxidation of methane related to a change in sedimentation rate[J]. Geochimica et Cosmochimica Acta, 2005, 69(16): 4117-4126.

[74] Hilligsøe K M, Jensen J B, Ferdelman T G, et al. Methane fluxes in marine sediments quantified through core analyses and seismo-acoustic mapping (Bornholm Basin, Baltic Sea)[J]. Geochimica et Cosmochimica Acta, 2018, 239: 255-274.

[75] Blanchet C L, Thouveny N, Vidal L, et al. Terrigenous input response to glacial/interglacial climatic variations over southern Baja California: A rock magnetic approach[J]. Quaternary Science Reviews, 2007, 26(25/26/27/28): 3118-3133.

[76] Liu J, Zhu R X, Roberts A P, et al. High-resolution analysis of early diagenetic effects on magnetic minerals in post-middle-Holocene continental shelf sediments from the Korea Strait[J]. Journal of Geophysical Research: Solid Earth, 2004, 109(B3): B03103.

[77] Roberts A P. Magnetic mineral diagenesis[J]. Earth-Science Reviews, 2015, 151: 1-47.

[78] Zheng Y, Kissel C, Zheng H B, et al. Sedimentation on the inner shelf of the East China Sea: Magnetic properties, diagenesis and paleoclimate implications[J]. Marine Geology, 2010, 268 (1/2/3/4): 34-42.

[79] Chen T, Wang Z H, Wu X X, et al. Magnetic properties of tidal flat sediments on the Yangtze coast, China: Early diagenetic alteration and implications[J]. The Holocene, 2015, 25(5): 832-843.

[80] Ge C, Zhang W G, Dong C Y, et al. Magnetic mineral diagenesis in the river-dominated inner shelf of the East China Sea, China[J]. Journal of Geophysical Research: Solid Earth, 2015, 120(7): 4720-4733.

[81] Zheng Y, Zheng H B, Kissel C, et al. Sedimentation rate control on diagenesis, East China Sea sediments[J]. Physics of the Earth and Planetary Interiors, 2011, 187(3/4): 301-309.

[82] Roberts A P, Zhao X, Harrison R J, et al. Signatures of reductive magnetic mineral diagenesis from unmixing of first-order reversal curves [J]. Journal of Geophysical Research: Solid Earth, 2018, 123(6): 4500-4522.

[83] 徐方建,李安春,肖尚斌,等. 末次冰消期以来东海内陆架古环境演化[J]. 沉积学报,2009,27(1):118-127.[Xu Fangjian, Li Anchun, Xiao Shangbin, et al. Paleoenvironmental evolution in the inner shelf of the East China Sea since the last deglaciation [J]. Acta Sedimentologica Sinica, 2009, 27 (1): 118-127.]

[84] Liu X T, Li A C, Dong J, et al. Nonevaporative origin for gypsum in mud sediments from the East China Sea shelf[J]. Marine Chemistry, 2018, 205: 90-97.

[85] 石学法,刘升发,乔淑卿,等. 中国东部近海沉积物地球化学:分布特征、控制因素与古气候记录[J]. 矿物岩石地球化学通报, 2015, 34 (5): 885-894.[Shi Xuefa, Liu Shengfa, Qiao Shuqing, et al. Geochemical characteristics, controlling factor and record of paleoclimate in sediments from eastern China seas [J]. Bulletin of Mineralogy, Petrology and Geochemistry, 2015, 34(5): 885-894.]

[86] 杨守业,韦刚健,石学法. 地球化学方法示踪东亚大陆边缘源汇沉积过程与环境演变[J]. 矿物岩石地球化学通报,2015,34(5):902-910.[Yang Shouye, Wei Gangjian, Shi Xuefa. Geochemical approaches of tracing source-to-sink sediment processes and environmental changes at the East Asian continental margin[J]. Bulletin of Mineralogy, Petrology and Geochemistry, 2015, 34(5): 902-910.]

[87] 石学法,胡利民,乔淑卿,等. 中国东部陆架海沉积有机碳研究进展:来源、输运与埋藏[J]. 海洋科学进展,2016,34(3):313-327.[Shi Xuefa, Hu Limin, Qiao Shuqing, et al. Progress in research of sedimentary organic carbon in the East China Sea: Sources, dispersal and sequestration[J]. Advances in Marine Science, 2016, 34(3): 313-327.]

[88] 刘健,秦华峰,孔祥淮,等. 黄东海陆架及朝鲜海峡泥质沉积物的磁学特征比较研究[J]. 第四纪研究,2007,27(6):1031-1039.[Liu Jian, Qin Huafeng, Kong Xianghuai, et al. Comparative researches on the magnetic properties of muddy sediments from the Yellow Sea and East China Sea shelves and the Korea Strait[J]. Quaternary Sciences, 2007, 27(6): 1031-1039.]

[89] Yang S Y, Wang Z B, Dou Y G, et al. A review of sedimentation since the Last Glacial Maximum on the continental shelf of eastern China [J]. Geological Society, London, Memoirs, 2014, 41: 293-303.

[90] Liu J P, Li A C, Xu K H, et al. Sedimentary features of the Yangtze River-derived along-shelf clinoform deposit in the East China Sea[J]. Continental Shelf Research, 2006, 26(17/18): 2141-2156.

[91] Liu X T, Li A C, Dong J, et al. Provenance discrimination of sediments in the Zhejiang-Fujian mud belt, East China Sea: Implications for the development of the mud depocenter[J]. Journal of Asian Earth Sciences, 2018, 151: 1-15.

[92] Gao S. Holocene shelf-coastal sedimentary systems associated with the Changjiang River: an overview[J]. Acta Oceanologica

Sinica, 2013, 32(12): 4-12.

[93] Gao S, Collins M B. Holocene sedimentary systems on continental shelves[J]. Marine Geology, 2014, 352: 268-294.

[94] Zhang K D, Li A C, Huang P, et al. Sedimentary responses to the cross-shelf transport of terrigenous material on the East China Sea continental shelf[J]. Sedimentary Geology, 2019, 384: 50-59.

[95] Qiao S Q, Shi X F, Wang G Q, et al. Sediment accumulation and budget in the Bohai Sea, Yellow Sea and East China Sea [J]. Marine Geology, 2017, 390: 270-281.

[96] Dong J, Li A C, Liu X T, et al. Sea-level oscillations in the East China Sea and their implications for global seawater redistribution during 14. 0-10. 0 kyr BP[J]. Palaeogeography, Palaeoclimatology, Palaeoecology, 2018, 511: 298-308.

[97] Ge H M, Zhang C L, Versteegh G J M, et al. Evolution of the East China Sea sedimentary environment in the past 14 kyr: Insights from tetraethers-based proxies[J]. Science China Earth Sciences, 2016, 59(5): 927-938.

[98] 王昆山,石学法,李珍,等. 东海DGKS9617岩心重矿物及自生黄铁矿记录[J]. 海洋地质与第四纪地质,2005,25(4):41-45.[Wang Kunshan, Shi Xuefa, Li Zhen, et al. Records of heavy mineral and authigenous pyrite in Core DGKS9617 from the East China Sea[J]. Marine Geology & Quaternary Geology, 2005, 25(4): 41-45.]

[99] Duan W M, Chen L R. Pyrite genesis during early diagenesis in Yellow Sea and East China Sea[J]. Science in China (Series B), 1994, 37(4): 502-512.

[100] Lin S, Huang K M, Chen S K. Organic carbon deposition and its control on iron sulfide formation of the southern East China Sea continental shelf sediments [J]. Continental Shelf Research, 2000, 20(4/5): 619-635.

[101] Zhu M X, Shi X N, Yang G P, et al. Formation and burial of pyrite and organic sulfur in mud sediments of the East China Sea inner shelf: Constraints from solid-phase sulfur speciation and stable sulfur isotope [J]. Continental Shelf Research, 2013, 54: 24-36.

[102] Zhao B, Yao P, Bianchi T S, et al. The role of reactive iron in the preservation of terrestrial organic carbon in estuarine sediments[J]. Journal of Geophysical Research: Biogeosciences, 2018, 123(12): 3556-3569.

[103] 郑妍,郑洪波,王可. 末次冰期以来东海内陆架沉积反映的海平面变化[J]. 同济大学学报(自然科学版),2010,38(9):1384-1386.[Zheng Yan, Zheng Hongbo, Wang Ke. History of sea level change since last glacial: Reflected by sedimentology of core from East China Sea inner shelf [J]. Journal of Tongji University (Natural Science), 2010, 38 (9): 1381-1386.]

[104] Kang X M, Liu S M, Zhang G L. Reduced inorganic sulfur in the sediments of the Yellow Sea and East China Sea[J]. Acta Oceanologica Sinica, 2014, 33(9): 100-108.

[105] Canfield D E, Raiswell R, Westrich J T, et al. The use of chromium reduction in the analysis of reduced inorganic sulfur in sediments and shales[J]. Chemical Geology, 1986, 54(1/2): 149-155.

[106] Diaz R, Moreira M, Mendoza U, et al. Early diagenesis of sulfur in a tropical upwelling system, Cabo Frio, southeastern Brazil[J]. Geology, 2012, 40(10): 879-882.

[107] Lin Z Y, Sun X M, Lu Y, et al. Stable isotope patterns of coexisting pyrite and gypsum indicating variable methane flow at a seep site of the Shenhu area, South China Sea[J]. Journal of Asian Earth Sciences, 2016, 123: 213-223.

[108] Holmkvist L, Kamyshny A, Jr, Brüchert V, et al. Sulfidization of lacustrine glacial clay upon Holocene marine transgression (Arkona Basin, Baltic Sea)[J]. Geochimica et Cosmochimica Acta, 2014, 142: 75-94.

[109] Li G X, Li P, Liu Y, et al. Sedimentary system response to the global sea level change in the East China Seas since the last glacial maximum [J]. Earth-Science Reviews, 2014, 139: 390-405.

[110] Gomes M L, Fike D A, Bergmann K D, et al. Environmental insights from high-resolution (SIMS) sulfur isotope analyses of sulfides in Proterozoic microbialites with diverse mat textures[J]. Geobiology, 2018, 16(1): 17-34.

[111] Zhao B, Yao P, Bianchi T S, et al. The remineralization of sedimentary organic carbon in different sedimentary regimes of the Yellow and East China Seas[J]. Chemical Geology, 2018, 495: 104-117.

[112] 刘喜停,颜佳新. 铁元素对海相沉积物早期成岩作用的影响[J]. 地球科学进展,2011,26(5):482-492.[Liu Xiting, Yan Jiaxin. Advances in the role of iron in marine sediments during early diagenesis[J]. Advances in Earth Science, 2011, 26(5): 482-492.]

[113] Zhang X, Lin C M, Li Y L, et al. Sealing mechanism for cap beds of shallow-biogenic gas reservoirs in the Qiantang River incised valley, China[J]. Continental Shelf Research, 2013, 69: 155-167.

[114] Peng X T, Guo Z X, Chen S, et al. Formation of carbonate pipes in the northern Okinawa Trough linked to strong sulfate exhaustion and iron supply[J]. Geochimica et Cosmochimica Acta, 2017, 205: 1-13.

[115] Liu J R, Izon G, Wang J S, et al. Vivianite formation in methane-rich deep-sea sediments from the South China Sea[J]. Biogeosciences, 2018, 15(20): 6329-6348.

Constraint of Sedimentary Processes on the Sulfur Isotope of Authigenic Pyrite

LIU XiTing[1], LI AnChun[2], MA ZhiXin[3], DONG Jiang[4], ZHANG KaiDi[2], XU FangJian[5], WANG HouJie[1]

1. College of Marine Geosciences, Key Laboratory of Submarine Geosciences and Prospecting Technology, Ocean University of China, Qingdao, Shandong 266100, China

2. Key Laboratory of Marine Geology and Environment, Institute of Oceanology, Chinese Academy of Sciences, Qingdao, Shandong 266071, China

3. Chengdu Center, China Geological Survey, Chengdu 610081, China

4. Key Laboratory of Marine Sedimentology and Environmental Geology, First Institute of Oceanography, Ministry of Natural Resources, Qingdao, Shandong 266061, China

5. School of Geosciences, China University of Petroleum (East China), Qingdao, Shandong 266580, China

Abstract: Authigenic pyrite is the main mineral specie of reduced sulfur in marine sediments. Its formation process is related to organic mineralization and affects the global C-S-Fe biogeochemical cycle. Sulfur isotope fractionation of authigenic pyrite is mainly controlled by microbial sulfate reduction, but recent studies have indicated that the local depositional environment also affects the composition of pyrite sulfur isotopes, especially in shallow depositional environments. In an unsteady shallow environment, physical reworking and bioturbation lead to reoxidation of sulfides formed in the sulfate reduction zone, which in turn affects the sulfur isotopes of pyrite. The sedimentation process in a shallow depositional environment is readily affected by paleoclimate and sea-level changes, which cause drastic fluctuations in sedimentation rate as well as instable input of, for instance, organic matter and active iron. This in turn affects the openness of the diagenetic system and ultimately affects the isotopic value of pyritic sulfur. In addition, any change in sedimentation rate also affects the movement of the sulfate-methane transition zone, resulting in the conversion of organic matter and anaerobic oxidation methane sulfate reduction, producing different sulfur isotope signals. The study of the sulfur isotopes of authigenic pyrite in the mud area of the inner shelf of the East China Sea provides a good example for depositional control on the formation of authigenic pyrite and its sulfur isotope composition. The sedimentary process of this area has been well studied, and its sediments have been shown to be enriched in authigenic pyrite and biogas (CH_4). Therefore, it is an ideal site for studying the sulfur cycle in a marginal sea, and is expected to provide a new perspective on the global C-S-Fe biogeochemical cycle.

Key words: pyrite; sulfur isotope; microbial sulfate reduction; sedimentary environment; East China Sea